

# Cryogenic Testing of Microwave Kinetic Inductance Detectors (MKIDS)

Paul Abers<sup>1</sup>, Philip Mauskopf<sup>2</sup> and Hamdi Mani<sup>3</sup> April 2017

## Abstract

We designed and constructed a cryostat setup for MKID detectors. The cryostat has four stages: 40K, 4K, 1K and 250mK. The 4K stage is used to cool various devices as well as a stepping stone for further cold stages. It is large enough to mount a few resonator packages, house the sorption cooler and to house the milliKelvin stage. The final stage, 250mK, is designed to house up to a six inch wafer, while being fully enclosed in a radiative shield. A Niobium MKID from Stanford was tested in our cryostat setup for various temperatures and input powers in order to test our system and setup. Lastly, a homodyne noise characterization setup was designed for future testing.

\*This work was not supported by any organization

<sup>1</sup>P. Abers is an undergraduate at Barrett the Honors College at Arizona State University, Tempe, AZ 85281, USA

<sup>2</sup>P. Mauskopf is a Professor in the Department of Physics and Director of the Earth and Space Exploration Department, Arizona State University, Tempe, AZ 85281, USA

<sup>3</sup>H. Mani is a research technician with the Department of Earth and Space Exploration, Arizona State University, Tempe, AZ 85281, USA

## I. INTRODUCTION

The field of astronomy and astronomical observations has been steadily growing since the early 20th century. Astronomical observation techniques have advanced greatly from its origins in the naked eye and simple lens refraction telescopes. Modern techniques include large mirror telescopes (some of which are in space orbiting Earth), large radio interferometry and other various methods. A growing method for astronomy observations is Microwave Kinetic Inductance Detectors (MKIDs). MKIDs are detectors for microwave radiation that use kinetic inductance, a phenomenon that occurs in certain materials under superconducting conditions. The advantages of MKIDs is that they are quite sensitive to small amounts of incoming radiation. Many objects in space are cold, on the order of tens of Kelvin, and thus their emissions are weak. It requires very sensitive instrumentation to detect their emissions and gather data. MKIDs are able to detect small traces of incoming radiation, and they have possibly more uses that are currently being investigated. In our lab we needed to design and construct a testbed setup for MKIDs, in order to determine and test their capabilities. Since MKIDs rely on the material to be superconducting, our testbed must reach subKelvin temperatures. The critical temperature for the MKIDs I am working with is 9K (Niobium). Therefore, our testbed setup must be able to house an MKID package that reaches subKelvin temperatures (below 500mK). Reaching subKelvin temperatures requires a solid understanding of heat transfer physics and engineering. The main proponents of thermal loading are conduction, radiation and thermal mass. It is important for our design to minimize these factors while maintaining structural integrity and ease of use for the system.

## II. CRYOSTAT TEST-BED SETUP FOR 4K STAGE

### A. *Methodology*

The goal for the cryostat is to be able to reach sub 4 Kelvin temperatures on the second stage while maintaining a large plate to attach detectors and devices to in order to test the noise of MKIDS. This is achieved by minimizing thermal loading onto the second stage and having good heat strapping from the pulse tube refrigerator's cold heads to the stages. There are three main focuses for the thermal loading of the stages: Thermal Radiation, Thermal Conduction and Thermal Mass. Some of the parts were already ordered and machined upon the beginning of this project, and thus the thermal mass of the setup was mostly fixed. Therefore, the focus of the construction was on thermal isolation and thermal shielding.

### B. Preliminary Cooldowns

The first step for the construction of the cryostat was to test the performance of the pulse tube by creating a heat capacity map comparison with performance in our lab versus the expected performance based on Sumitomo's tests.



Fig. 1: 4K and 40K Coldhead Test Setup (Shell Not Installed)



Fig. 2: 4k and 40K Coldhead Test Setup (Aluminum Tape Shell Installed to 40k Stage)

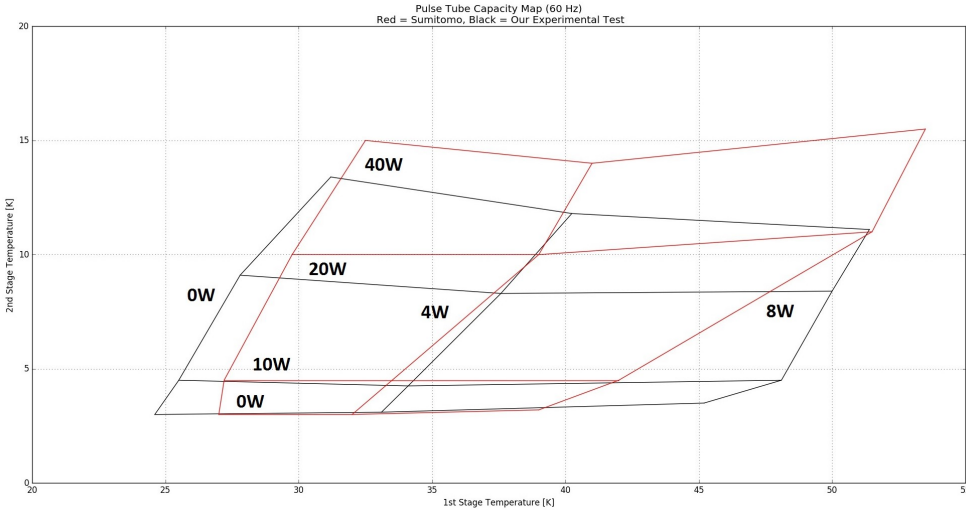


Fig. 3: Coldhead Cooling Capacity Map (Sumitomo in Red and Our Test in Black)

As can be seen from figure 3, the cold heads performed as expected with nothing added to the cold stages. The next step was to test the cryostat with the first stage attached. Adding the first stage to the cryostat created various reasons for thermal loading. First off, the larger amount of mass means the cold head has more material to cooldown. Second, the larger stage has a greater absorption of thermal radiation. The thermal radiation experienced by an object goes as the surface area encountering the radiation. When the first stage was added, the surface area was immensely increased. Furthermore, the supporting struts between the first stage and outer stage is a thermal connection that allows heat to flow via conduction. To limit these effects on our cooldown we used several strategies. To help limit the thermal radiation effect from the cooldown we added multi layer insulation (MLI). The equation for the heat transferred via radiation is:

$$Q = \epsilon\sigma T^4 \quad (1)$$

Where  $Q$  is the heat transferred,  $\epsilon$  is the emissivity of an object,  $\sigma$  is the Stefan-Boltzmann constant and  $T$  is the temperature. Our first stage material is unpolished Aluminum, which has a low emissivity because it is not shiny. The Aluminized Mylar has a very high emissivity. To further decrease the factor of radiative heating we used 2 layers of MLI. Each layer had one layer of Aluminized Mylar and then a subsequent layer of gauze netting to insulate each layer from the next. The next step was minimizing the effect of the supporting struts. Since the struts are

in contact with both the 40K and 300K stages, the thermal conduction factor is the dominating term here. The equation for heat transfer via conduction is:

$$\delta Q = \frac{Ak(T)\delta T}{L} \quad (2)$$

Once again Q is heat transferred, A is the cross-sectional area, k is the thermal conductivity factor, T is the temperature and L is the length. We have to integrate this equation to find the heat transferred across the supports from two different temperatures. To minimize the heat transferred, one can decrease the cross sectional area, increase the length and/or decrease the thermal conductivity. Stainless steel offers superior mechanical strength while also offering low thermal conductivity. After adding the four, hollow stainless steel struts and the MLI to the first stage, we ran another cooldown.

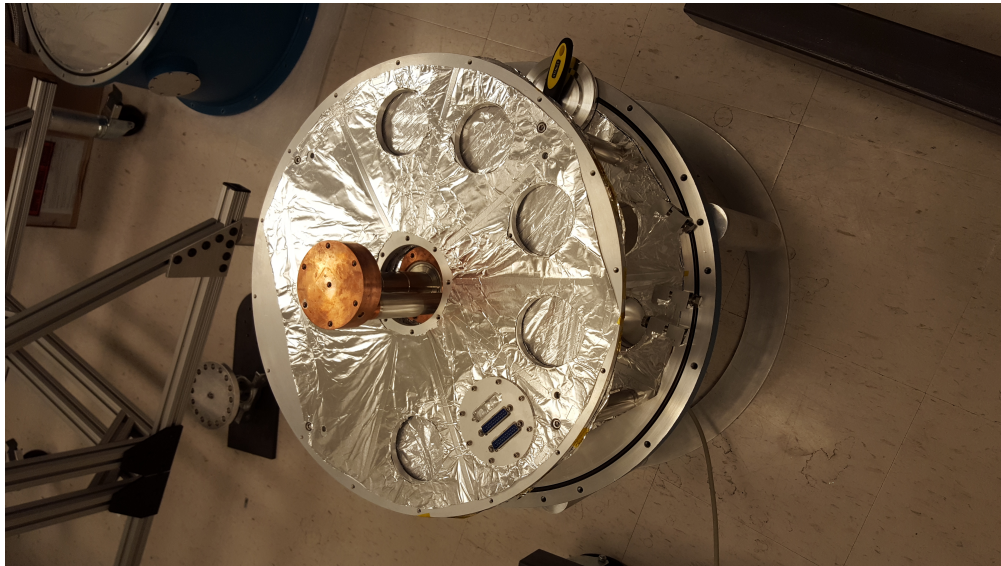


Fig. 4: First Stage Initial Cooldown (Plate Installed)

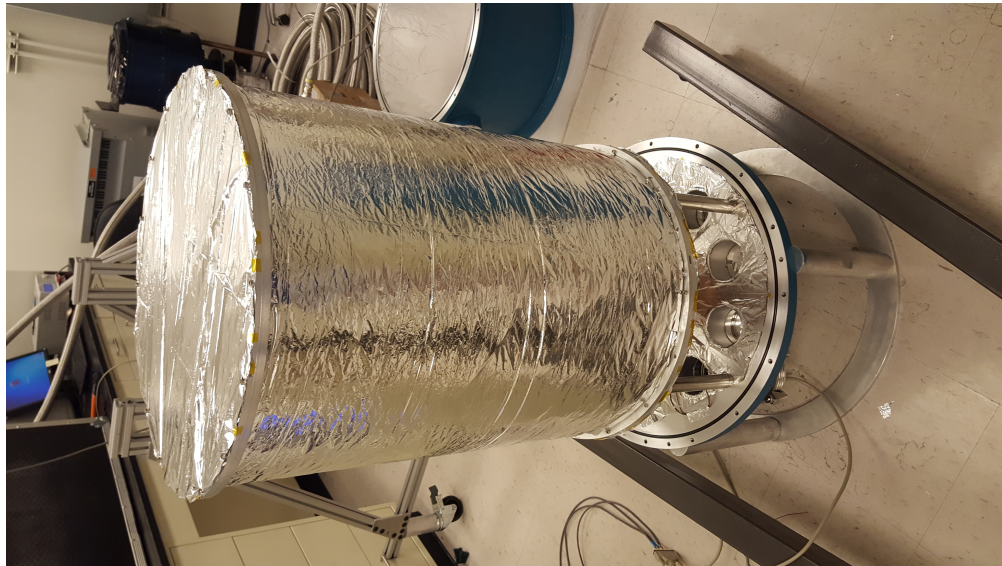


Fig. 5: First Stage Initial Cooldown (Radiative Shell Installed)

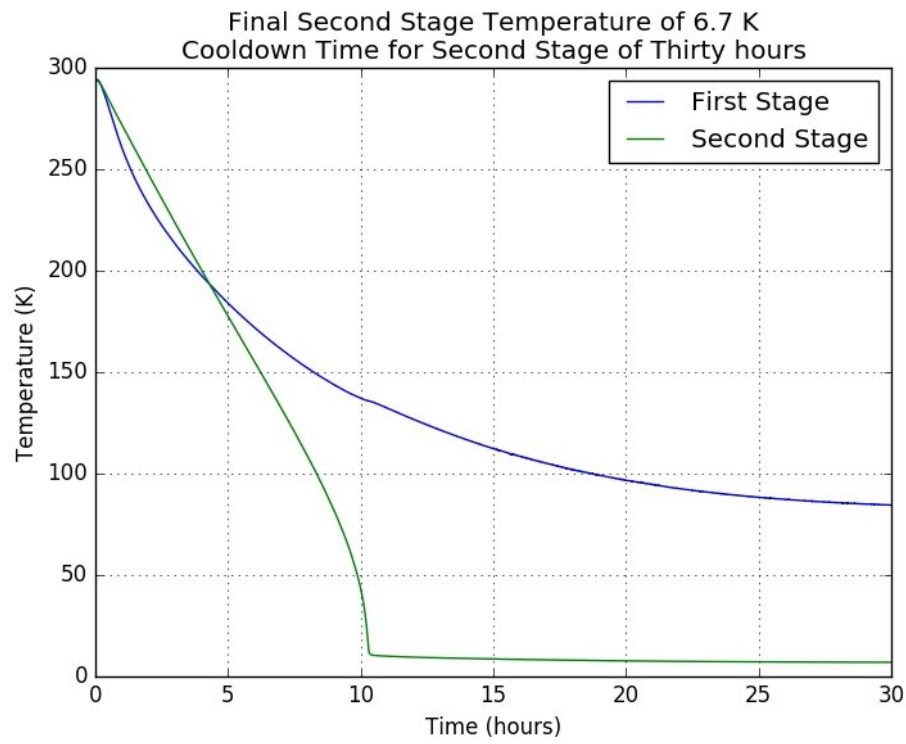


Fig. 6: Cooling Curve for Initial Cooldown of First Stage

The cooldown only reached a base temperature of about 7K for the second stage. The thermal loading from radiation and conduction was apparently too much to handle for the second stage.

We decided to increase the number of layers of MLI on the first stage to ten layers. We also measured the length and thickness of the stainless steel rods and calculated the conductive heat loading.

Integrating equation 2 yields:

$$Q = \frac{AK}{L} \quad (3)$$

where K is the value of the integral of thermal conductivity from the colder temperature to the warmer temperature. The cross sectional area of the tube is equal to the outer radius area minus the inner radius area (the supports are hollow).

$$A = \pi r^2 - \pi(r-t)^2 \quad (3)$$

The power transferred by the stainless steel supports via the 300K stage to the 40K stage was calculated to be 22W and the power transferred via the 40K stage to the 4K stage was calculated to be 1W. Data collected and reported by Jacob Kooi at Caltech was used to determine the K value in equation 3.<sup>1</sup> This corresponds with a second stage temperature of about 7K based on our capacity map we created in figure 3, and our cooldown resulted in a final temperature of about 7K. We sent the rods to be machined such that the thickness of the walls was reduced from 2 mm to 10 mil. This decreased the expected power transferred from 22W and 1W to 3W and .1W. Along with thinning the walls, two layers of MLI was added to the supports to decrease radiative heat loading on the supports. Next, we ran a full cooldown with the sorption fridge installed, as well as the full first and second stages. The resulting cooldown was as follows:

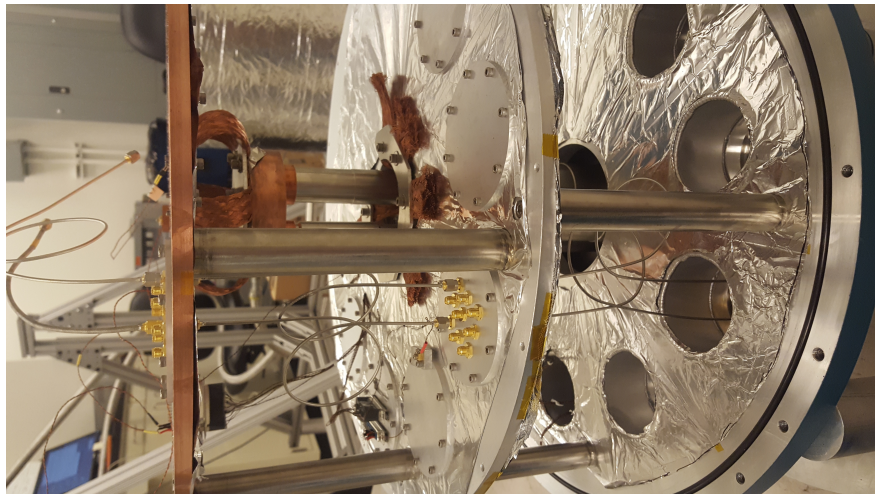


Fig. 7: Second Stage Initial Cooldown Setup



Fig. 8: Second Stage Initial Cooldown Setup with Second Stage Shell Installed

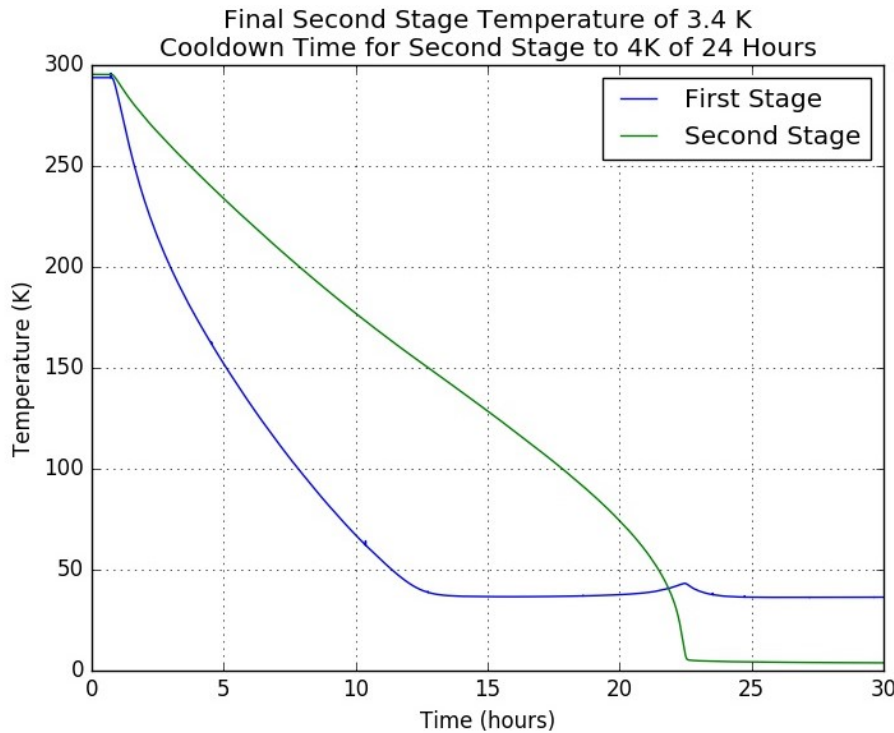


Fig. 9: Cooldown Curve for Second Stage Setup

With the MLI and the thinned stainless steel supports, we were able to reach our goal of below 4K for the second stage. At this point, the cryostat was ready to be used as a testbed for certain devices and detectors. The MLI is necessary for decreasing radiative heat loading to reach colder temperatures, but the downside is that it slows the vacuum pumping of the system. The

MLI can trap water vapor and air inside, and subsequently outgasses as the system is pumped on. However, once the cryostat reaches 77K during the cooldown, cryopumping begins and the outgassing is no longer a worry. Cryopumping is when the temperature within the cryostat reaches a cold enough temperature that the air molecules liquefy or freeze. Seventy-seven Kelvin is the temperature at which Nitrogen turns to a liquid and below 63 Kelvin Nitrogen freezes. Since our atmosphere is approximately three quarters Nitrogen, once we reach a temperature of 77K most of the remaining air inside the cryostat changes phase out of the gaseous phase and into liquids or solids.

### C. Final Test Cooldown

Occasional tweaks were made to the setup to attempt to reach colder and colder temperatures. The 4K plate was gold plated to increase emissivity and thermal contact for cooling. Eventually, we reached base temperatures of about 2.25K for the final stage. This was reached with everything installed, sorption fridge added and with devices added to the final stage for testing. The final setup consisted of 10 layers of MLI on the both the first and second stage shells, 8 layers on the first stage plate, 2 layers on the second stage plate and 4 layers on both the covers of the first and second stages. One layer of mylar was also placed on the inside of the 300K and 40K stages.

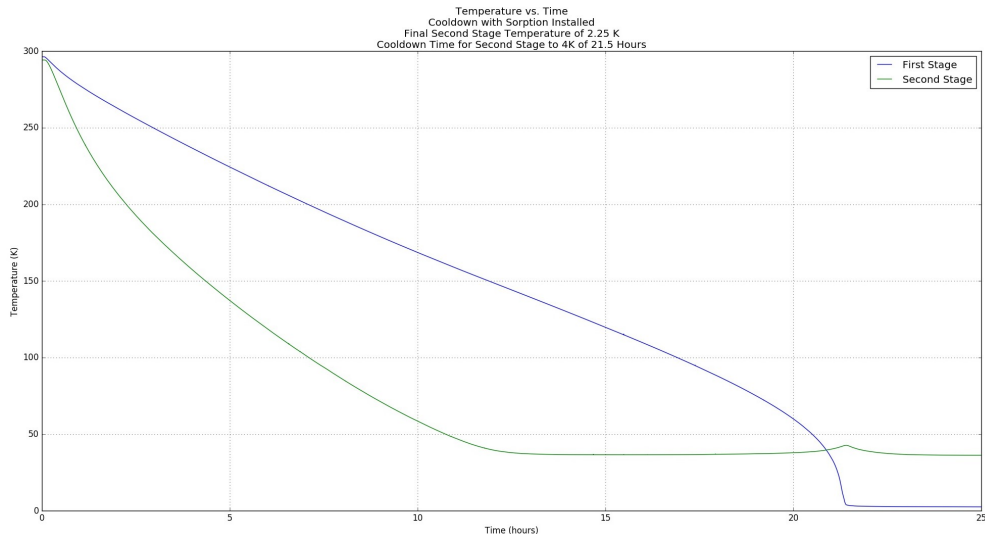


Fig. 10: Cooldown Curve for Final 4K Setup with Sorption and Devices Installed

### III. CRYOSTAT TEST-BED SETUP FOR MILLIKELVIN STAGE

Once we were able to cool the 4K stage down successfully with the sorption fridge installed, the next step was to design a milliKelvin stage that cools to 250mK. The requirements for the 250mK stage are that it must be able to house a six inch wafer detector, have a protective radiative shell, and reach at least a temperature of 300mK on the final (Ultracold, UC) stage. In order to design the milliKelvin stage we first looked at the heat transfer for various materials. The first material we tested was stainless steel. Using data collected by Jacob W Kooi at Caltech<sup>1</sup>, we calculated that the heat transfer from three supports from the 4K to the 1K (Intercold, IC) stage was too much. The next material we looked into was PocoGraphite<sup>tm</sup>. A paper by Adam L. Woodcraft and others collected data for the thermal conductivity of the material in the subKelvin range.<sup>2</sup> Using the data from their tests, we created a python code to determine the heat transfer for various versions of supports for our stage. We found that with three legs the heat transfer could be minimized to below 30 microWatts on the IC stage and below 1 microWatt on the UC stage. Our sorption fridge can handle a heat load of 40 microWatts to the IC stage and 3 microWatts to the UC stage. We decided that the PocoGraphite<sup>tm</sup> material was the best option, with a structure for the legs of an L-bracket to minimize the cross-sectional heat transfer area (see eqn 3). Unfortunately, the price of PocoGraphit<sup>tm</sup> was too much. Instead, we used another carbon fiber material that was more affordable, but with the same L-brackey design. Small, square pieces of aluminum are used in the design to attach to the IC and UC stages and to the carbon fiber supports. The final design of the milliKelvin stage is shown below.

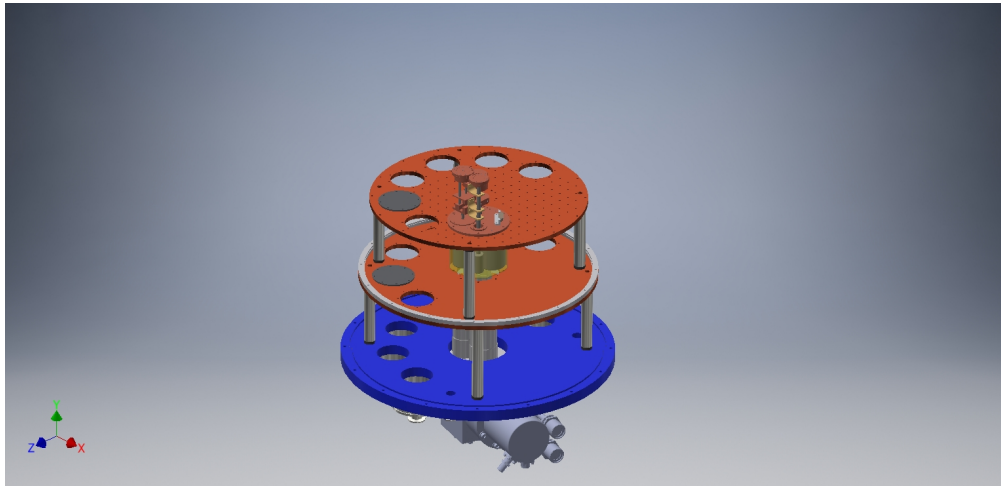


Fig. 11: SolidWorks Design of Cryostat up to 4K Stage

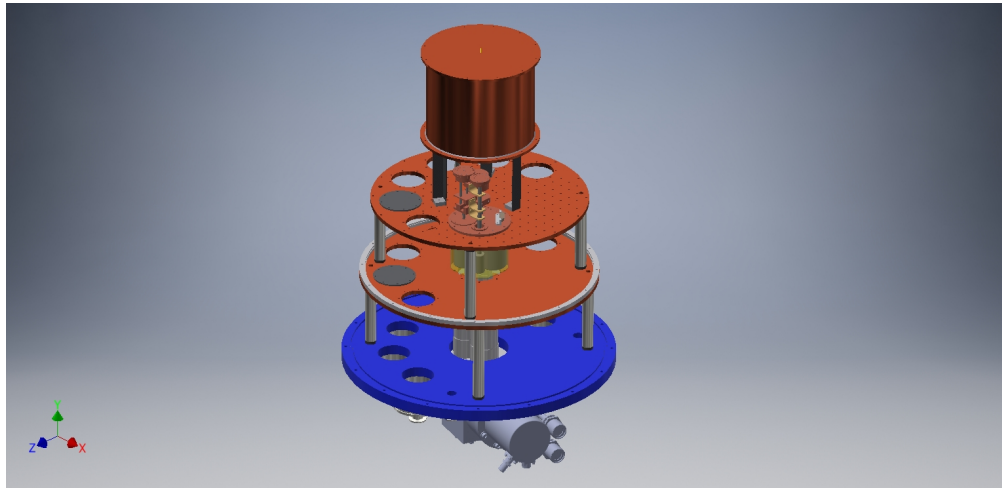


Fig. 12: SolidWorks Design of Cryostat with milliKelvin Stage Included

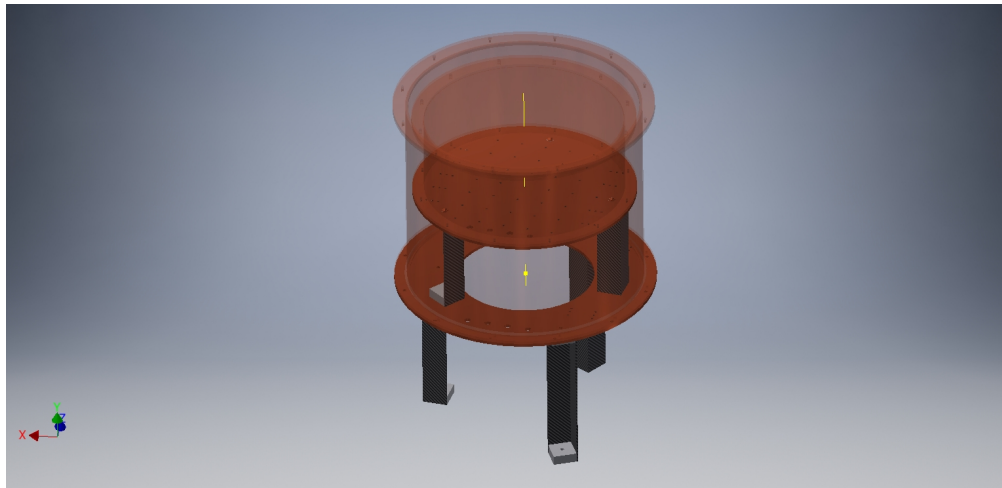


Fig. 13: SolidWorks Design of milliKelvin Stage

The performance of the milliKelvin stage was not able to be tested due to long lead times on construction of various parts.

#### IV. MKID THEORY

One major purpose of MKIDs is their ability to detect small amounts of photons. An MKID is a detector that has one or more parallel LC circuits that are composed of superconducting material. The detector must be placed in a cryostat that cools the device below its material's

critical temperature ( $T_c$ ). Once the material has passed its  $T_c$ , the material starts creating cooper pairs. In the simplest form, cooper pairs can be described as the pairing of two electrons. Cooper pairs are what gives superconductors their enhanced conductivity properties. Superconductors have essentially zero electrical resistance, which makes them a powerful tool for circuits. An MKID can be used as a photon detector because the material has a large number of coopers as the entire material is below the critical temperature of its material. Then, an incoming photon from some source comes into contact with the detector. Wherever the photon comes into contact with the MKID, it heats up that specific location on the detector. The spot that was hit by the photon then surpasses its  $T_c$  and a local cooper pair is broken where the photon hit. This causes the overall inductance of the material to decrease, as the inductance of an MKID is defined as:

$$L_K = L_{K0} \left(1 + \left(\frac{I}{I_*}\right)^2\right) \quad (4)$$

where  $L_{K0}$  is the kinetic inductance with no current through the material,  $L_K$  is the kinetic inductance of the material,  $I$  is the current through the material and  $I_*$  is an intrinsic property of the material.  $L_{K0}$  is calculated from the equation:

$$L_{K0} = \frac{ml}{ne^2 A} \quad (5)$$

where  $n$  is the number density of cooper pairs in the material. Thus, the kinetic inductance of the material is inversely proportional to the number of cooper pairs of the material. Which leads to the fact that the resonant frequency of the detector shifts down when light shines upon the detector, because resonant frequency of an LC circuit is:

$$\omega_o = \frac{1}{\sqrt{LC}} \quad (6)$$

where  $L$  is the inductance of the circuit and  $C$  is the capacitance. Thus, it becomes evident that the detector was hit with incoming photons because we can view a down-shift in its resonant frequency. Equations 4, 5 and 6 were pulled from Edward Schroeder's paper<sup>3</sup>.

## V. RESONANCE SHIFT DUE TO ULTRA COLD STAGE TEMPERATURE

Here, the temperature on the ultra cold stage was varied, causing the resonance shift of the MKID. The temperature was varied from 5.4K to 285mK, and the S21 data was gathered from

a vector network analyzer (VNA).  $S_{21}$  is the scattering parameter from the second port as compared to the first port.  $S_{21}$  is simply the forward voltage gain of the circuit. Therefore,  $S_{21}$  is measured by the VNA as  $V_2/V_1$ . If there is no voltage loss in the circuit (i.e.  $V_2$  equals  $V_1$ ), then  $S_{21}$  would just be equal to 1. We used the following setup inside the cryostat to test a resonator given to us from Stanford University. The following figures demonstrate the setup and circuitry for the measurements of the  $S_{21}$  of the MKID:

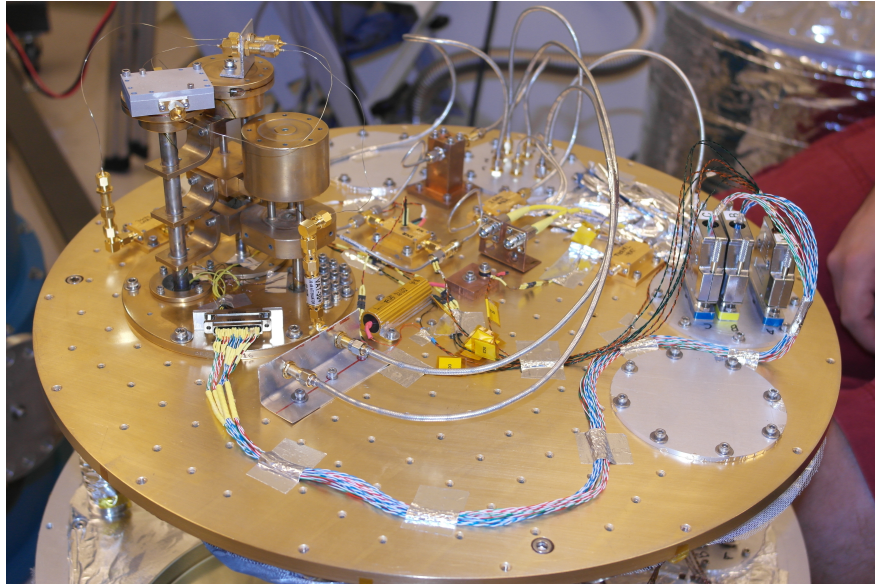


Fig. 14: Setup of Stanford Resonator on Ultra Cold stage in cryostat

Figure 14 shows the setup within the cryostat for testing the Stanford device. As can be seen from the figure, many devices are able to be cooled at once for the 4K stage of the cryostat. The Stanford device is the gray package in the upper left corner of the figure that is attached directly to the Ultra Cold stage. The Stanford MKID is just several parallel LC circuits coupled with a capacitor that are all in parallel with each other, as shown in figure 15. The circuit setup for measuring the device  $S_{21}$  is shown in figure 16. The input signal is attenuated 30 dB inside the cryostat, passed through the device and then amplified 30 dB via a low noise amplifier (LNA) inside the cryostat and then finally amplified 40 dB at room temperature before reaching the output port of the VNA. Our LNA was designed in house by Hamdi Mani. It is a 3GHz amplifier with 30 dB gain and minimal noise output. The LNA used in our system was constructed in house by Justin Mathewson. Once the device was cooled down, we measured the  $S_{21}$  versus frequency to find the resonances of the MKID.

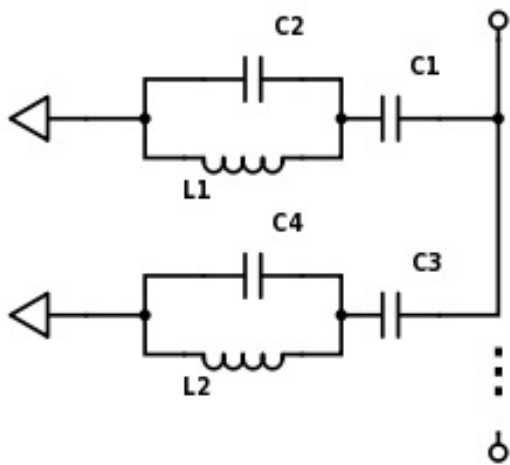


Fig. 15: Circuit Schematic for Stanford MKID Resonator

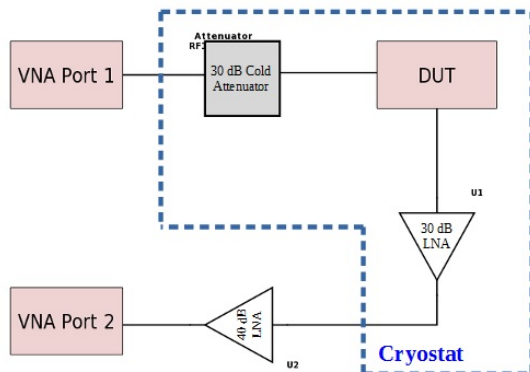


Fig. 16: Circuit Schematic for Setup of Device Under Test in Cryostat

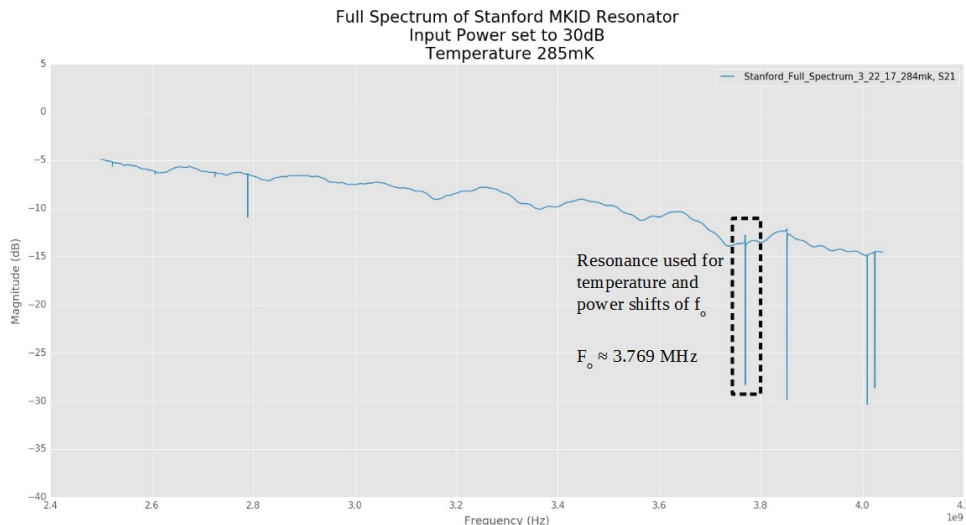


Fig. 17: S21 (dB) vs. Frequency (Hz)

After viewing the various resonances in the Stanford MKID in figure 17, I decided to use the resonant frequency at approximately 3.7MHz for our temperature and power shifts of the resonances. I chose this frequency because it was narrow and deep. Other resonances could also have been chosen, but it is important to choose the stronger performing resonances. In total,

there appears to be eight resonances, but only four of them are deep and narrow. I narrowed in on the 3.7MHz signal and then took data for the  $S_{21}$  versus frequency while varying the temperature of the UC stage from 5.4K to 285mK.

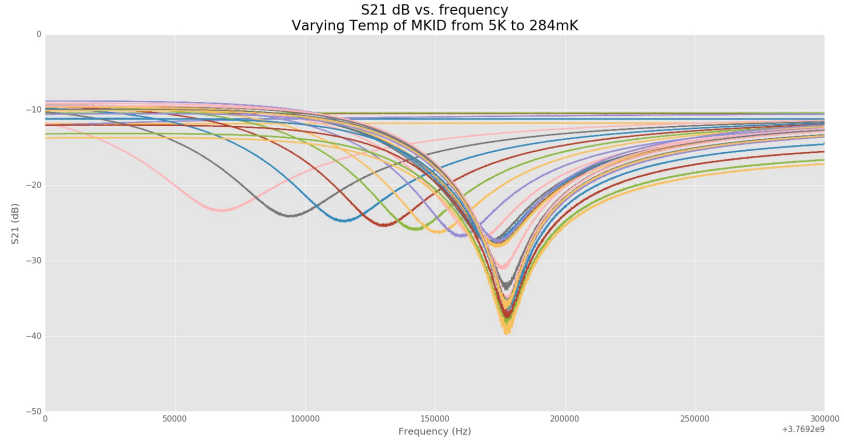


Fig. 18:  $S_{21}$  (dB) vs. Frequency (Hz)

As can be seen from figure 18, the resonant frequency shifts down in frequency with increasing the UC stage temperature, as expected. The resonances also shorten in depth with increasing UC stage temperature.

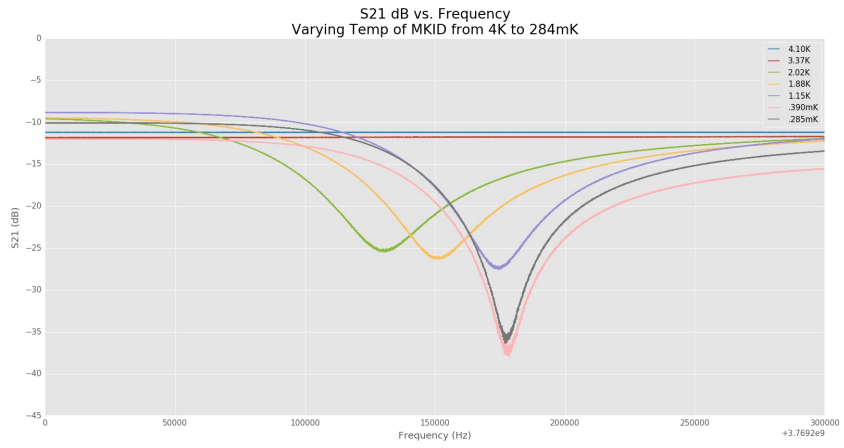


Fig. 19:  $S_{21}$  (dB) vs. Frequency (Hz)

Figure 19 emphasizes the temperature dependence of the MKID resonator. At 4 and 3 Kelvin the resonance are shifted out of the window of data collection. Therefore, we see no dip in the

$S_{21}$ . It can be seen as the device cools from 2 to 1.15 Kelvin that the resonant frequency and quality factor of the resonator keeps increasing with decreasing temperature. This is because more and more cooper pairs are being created as the device cools. Just after the device reaches 1.15K temperature, the quality factor greatly increases, as seen by the change in the curve from a temperature of 1.15K to a temperature of 390mK. To determine the quality factor,  $Q$ , and frequency of resonance, a python script was written. Initially, the data for  $S_{21}$  was plotted on the complex plane along with a theoretical model based on the following equation for  $s_{21}$ , as derived in Dr. Mauskopf's paper (in prep)<sup>4</sup>:

$$S_{21} = A \left( 1 - \frac{\frac{Q_r}{Q_c}}{1 + 2iQ_r \frac{f-f_o}{f_o}} \right) \quad (7)$$

Here,  $Q_r$  is the quality of the resonator,  $Q_c$  is the coupling quality factor and  $f_o$  is the resonant frequency. To determine the initial guesses for  $A$ ,  $Q_r$ ,  $Q_c$  and  $f_o$  we used a few different methods.  $A$  is the offset amplitude and is roughly the value of the magnitude for  $S_{21}$  for the initial frequency of the sweep.  $Q_r$  is  $f_o$  divided by  $\delta f_{3\text{db}}$ ,  $Q_c$  is assumed to be  $Q_r$  and  $f_o$  can be determined by the graph of  $S_{\text{db}}$  versus frequency.

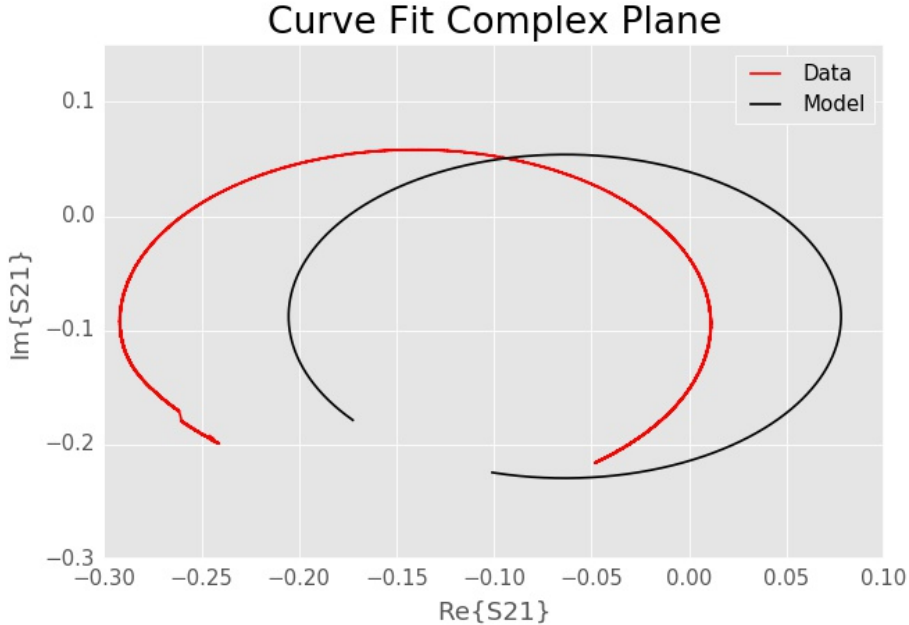


Fig. 20:  $S_{21}$  (dB) vs. Frequency (Hz)

After a little fine tuning to the input parameters to the model equation to closer match the model to data in figure 19, the input parameters are then used in a more in depth curve fit code for the db of  $S_{21}$  versus frequency. The code for the final curve fit was provided by Sean Bryan and it takes initial guesses (which need to be in the right ballpark) and then iteratively runs through a least squares fit to determine the values to greater accuracy. The result for the curve fit at a temperature of 439mK is shown in figures 21 and 22.

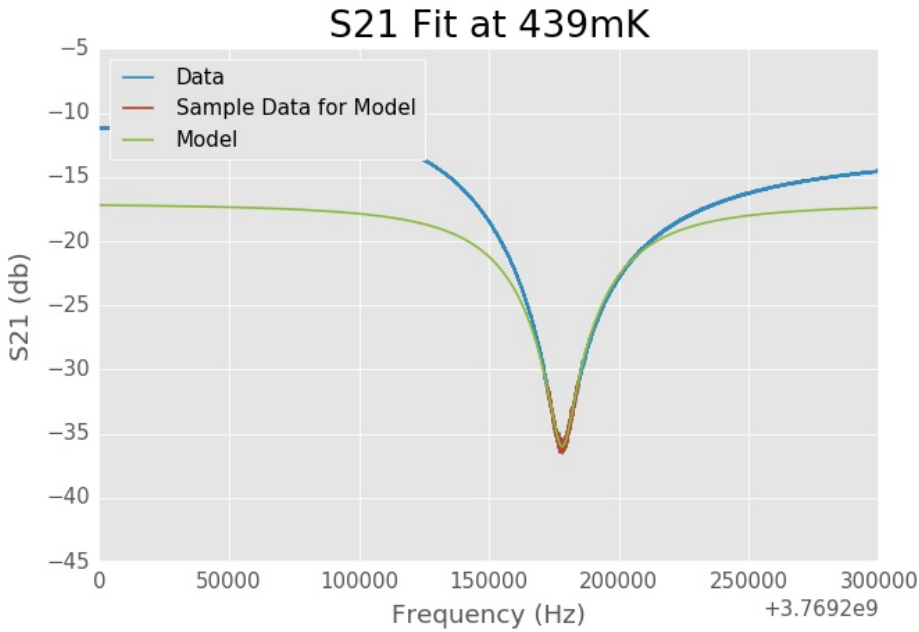


Fig. 21: S<sub>21</sub> (dB) vs. Frequency (Hz) at 439mK

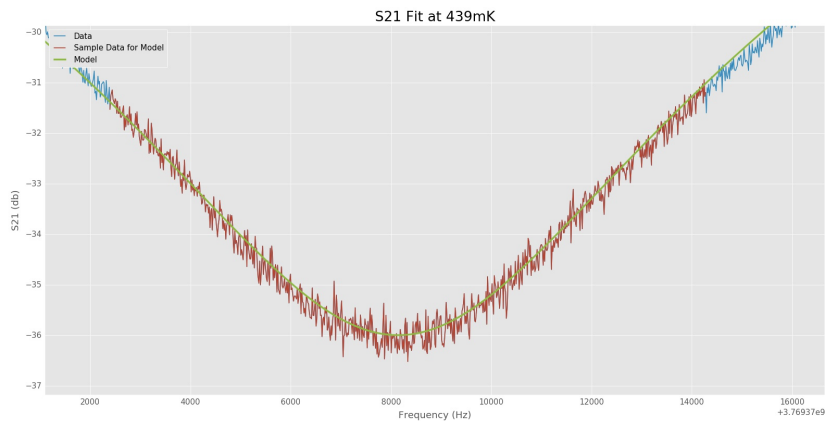


Fig. 22: S<sub>21</sub> (dB) vs. Frequency (Hz) at 439mK

Along with the graph seen in figure 21, the python code also determines the best fit values for  $Q_r$ ,  $Q_c$  and  $f_o$ . The previously described method was used to determine the quality factor and resonant frequency of the MKID at various temperatures. The intrinsic quality factor in the device can also be calculated,  $Q_i$ , from the results of  $Q_r$  and  $Q_c$ . (Equation 8 gathered from Edward Schroeder's paper<sup>3</sup>)

$$\frac{1}{Q_i} = \frac{1}{Q_r} + \frac{1}{Q_c} \quad (8)$$

TABLE I: Quality Factor and Resonant Frequency for Varied Stage Temperature

Temperature (K)	$Q_r$ (e4)	$Q_c$ (e4)	$Q_i$ (e4)	Resonant Frequency (GHz)
2.28	3.68	5.18	12.7	3.769269
2.12	3.71	5.28	12.4	3.769316
2.03	3.91	5.29	14.9	3.769331
1.88	4.03	5.31	16.8	3.769352
1.52	4.19	5.34	19.5	3.769372
1.25	4.49	5.76	20.5	3.769374
0.952	4.80	5.71	30.4	3.769376
0.776	4.86	5.56	38.4	3.769376
0.439	5.13	5.78	46.0	3.769378
0.336	5.74	6.55	47.7	3.769378
0.296	7.56	8.89	50.2	3.769378
0.285	9.27	11.4	50.5	3.769378

Next, the quality factors and the resonant frequency were plotted versus temperature.

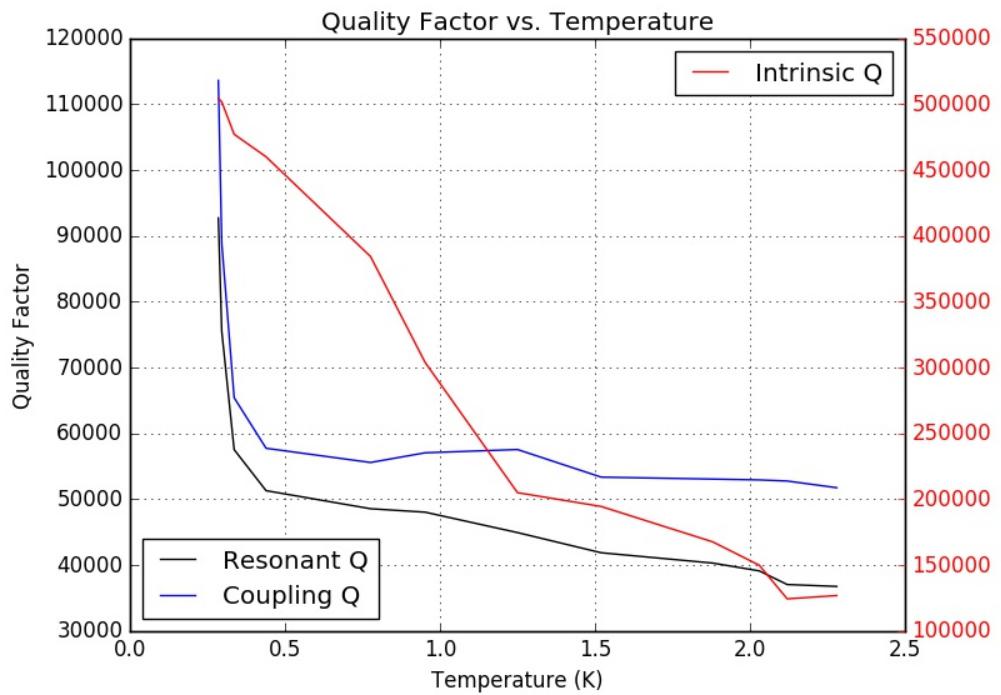


Fig. 23: Quality Factor vs. Temperature (K)

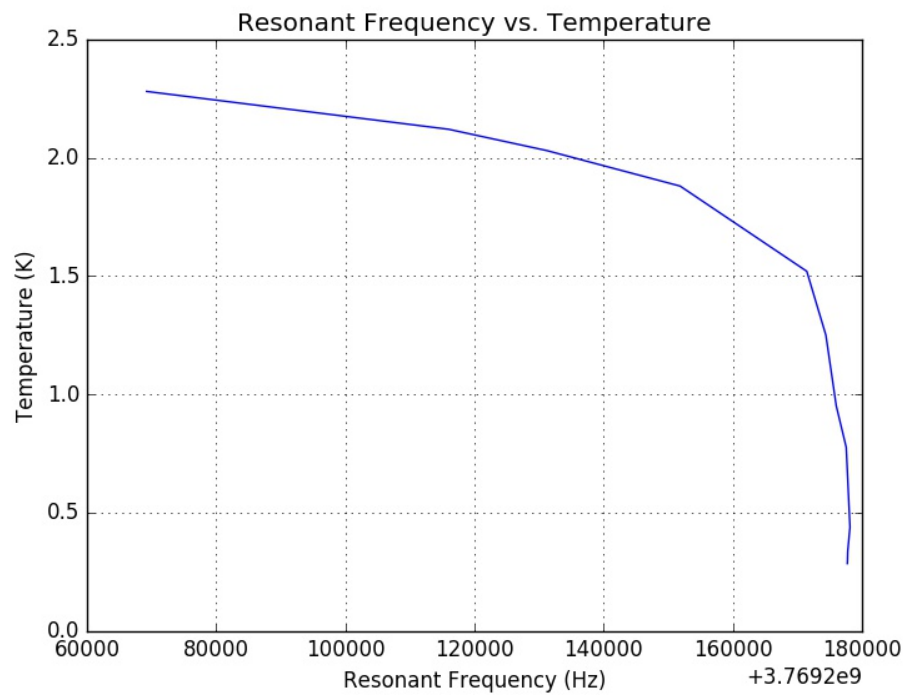


Fig. 24: Temperature (K) vs. Resonant Frequency (Hz)

As demonstrated in figure 23, the quality factor of the resonator is inversely proportional to temperature. In fact, the quality factors sees a large jump once the resonator reaches temperatures much lower than  $T_c$  (around 1.15K). The resonant frequency increases as temperature decreases, until it reaches its  $T_c$  and then the resonant frequency stabilizes around 3.769378 GHz.

## VI. RESONANCE SHIFT DUE TO INPUT POWER

The shifting of the resonant frequency due to heating the material can be caused by other methods as well. Changing the input power into the MKID can also cause the resonant frequency shift. This is due to the well known fact that increasing electrical power of a circuit increases its heat output. Therefore, by increasing the input power into the MKID, we are increasing the temperature of the MKID which breaks cooper pairs and decreases the resonant frequency (as discussed earlier with photons hitting the MKID). We used the same setup as in figure 16 to test the Stanford MKID with varied input power.

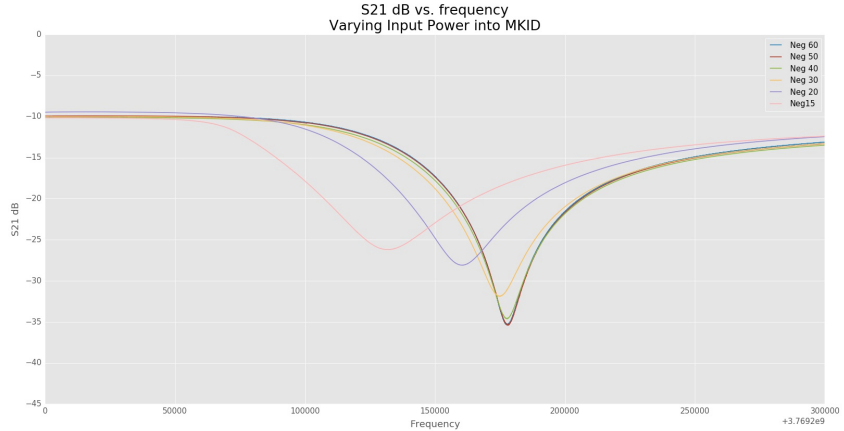


Fig. 25: S21 (dB) vs. Frequency (Hz) (Temperature of 285 mK)

As can be seen from figure 18, the resonant frequency shifts down in frequency with increasing the input power, as expected. The resonance also shorten in depth, which is also expected. To determine the quality factor,  $Q$ , and frequency of resonance, a python least squares fit was used via scipy. The  $Q$  and frequency at resonance was as follows:

TABLE II: Quality Factor and Resonant Frequency for Varied Input Power

Input Power (dB)	$(Q_r)$ (e4)	$(Q_c)$ (e4)	$(Q_i)$ (e4)	Resonant Frequency (GHz)
-60	5.70	6.45	49.0	3.769378
-50	5.66	6.41	48.4	3.769378
-40	5.53	6.35	42.3	3.769378
-30	4.79	5.68	30.6	3.769375
-20	3.80	4.76	18.8	3.769360
-15	3.25	4.36	12.8	3.769332

Again, quality factor and resonant frequency were plotted versus input power.

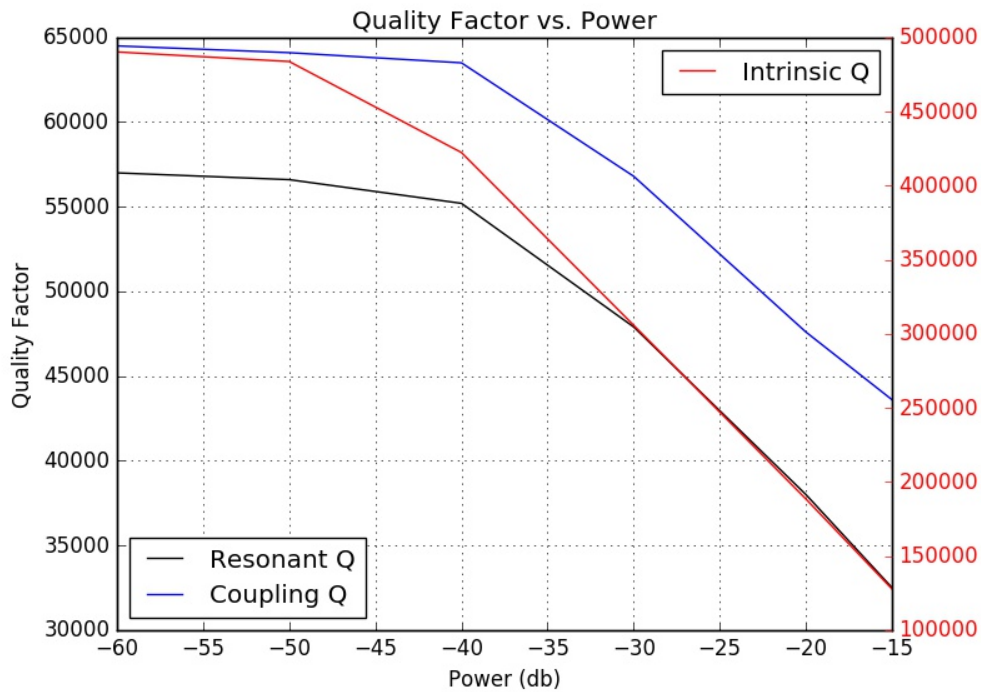


Fig. 26: Quality Factor vs. Input Power (db) (Temperature of 285 mK)

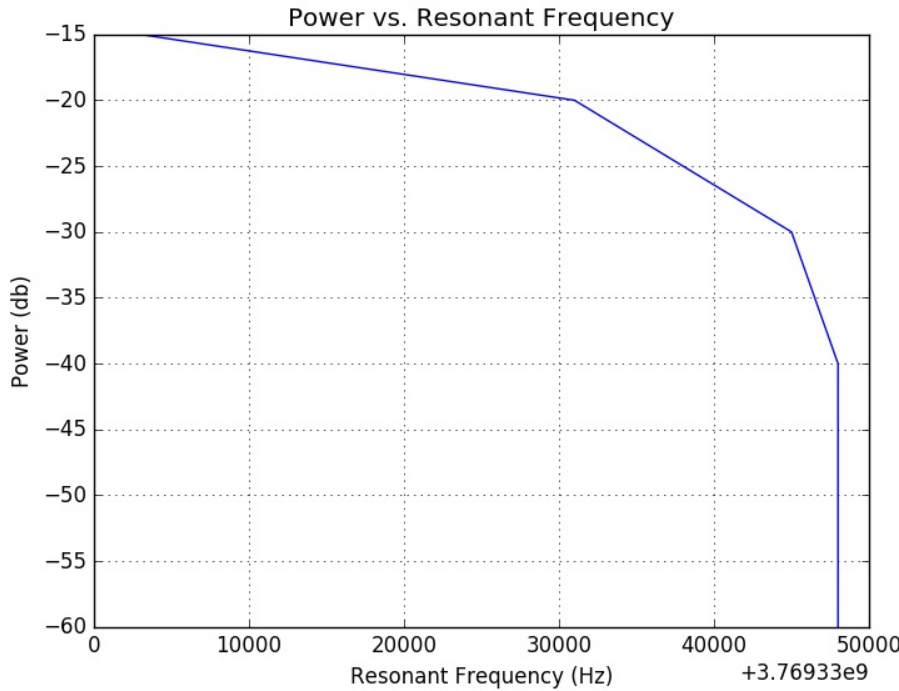


Fig. 27: Resonant Frequency (Hz) vs. Input Power (db) (Temperature of 285 mK)

As can be seen from figures 24 and 27, resonant frequency varies similarly with input power and temperature. This is because in both instances are changing temperature such that the device goes from outside its Tc (9K) to much below its Tc (285mK).

## VII. NOISE CHARACTERIZATION DATA

In order to characterize the noise of MKIDs, a new circuit is needed. A commonly used approach to characterizing the noise in MKIDs is to use a homodyne circuit setup. A homodyne setup is a circuit that uses a split rf input signal with half the signal acting as the local oscillator (LO) for an IQ modulator and the other half going through the system and acting as the radio frequency (RF) input of the IQ modulator. The benefits of this circuit setup is that since the signal is split in half, any noise within the source itself is cancelled out when the two halves are IQ modulated because any noise in the LO will also be present in the RF. Therefore, we do not have to worry about the noise in the source, and any noise found in the data is due to the device and not the source.

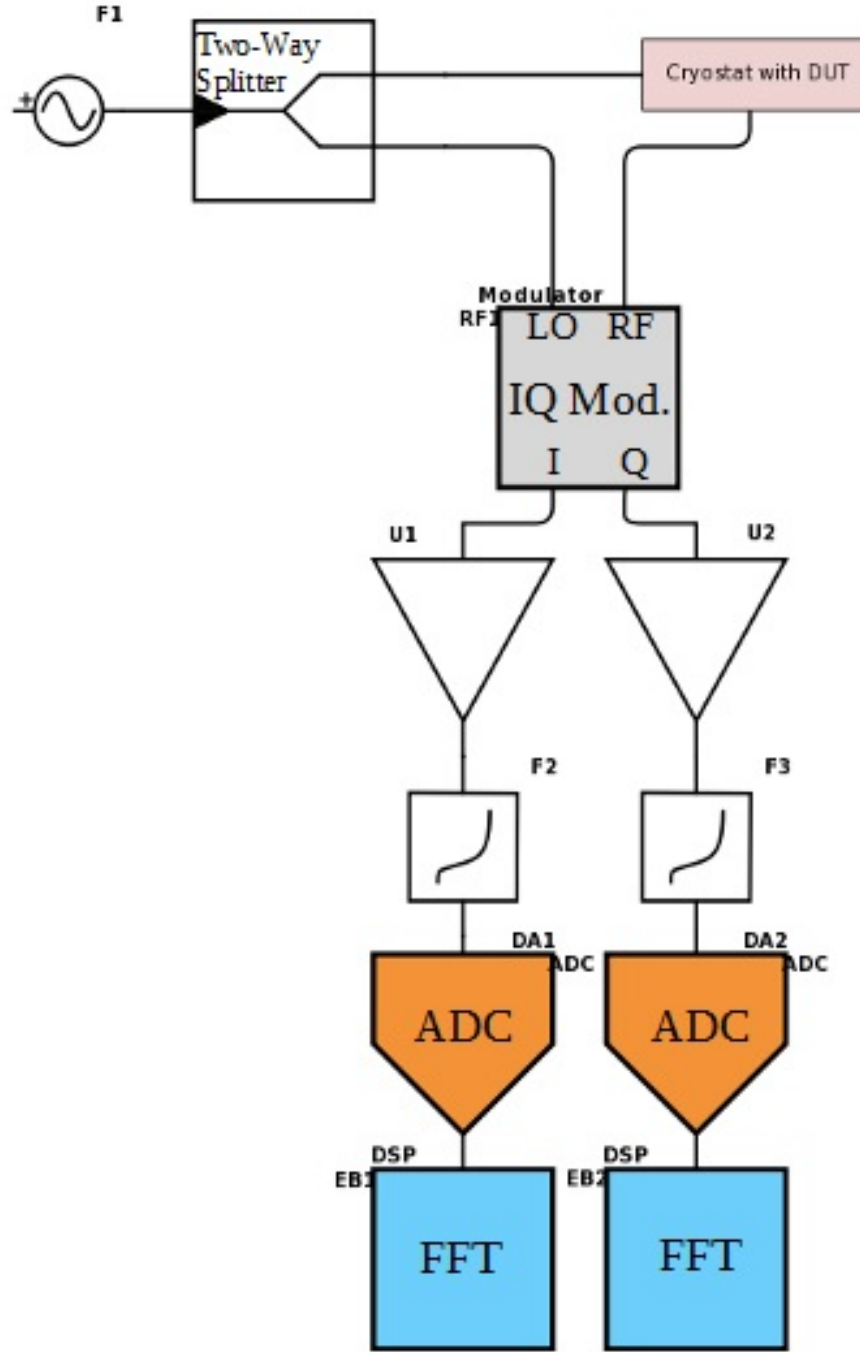


Fig. 28: Homodyne Circuit Design for MKID Noise Characterization

From figure 28, the source AC signal is split in two with equal power to each split. Half the split goes straight to the LO and the other half goes through the cryostat and through the device under test (DUT) and then into the RF input. The two signals are then IQ modulated. An IQ

modulator works as follows. First an LO must be sent to the modulator. The LO is what the RF is mixed with and is typically used as a tone frequency. The RF input is the signal that is being sampled. The RF and LO are mixed in the modulator and the output goes to I. Next, the LO is phase shifted 90 degrees and again mixed with the RF and the output goes to the Q output port. There are many benefits to an IQ modulator. For example, if a digitizer that someone has to sample a signal has a max sample rate of 256 MHz, but the signal is at a frequency of 1010MHz, then the digitizer is not fast enough to sample the data. However, if the RF, 1010 MHz, signal is sent to an IQ modulator along with a LO input of a 1000MHz tone, then the accompanying beat frequency of mixing the two signals is 10MHz. Therefore, the output of the IQ modulator at I and Q would have a frequency of 10MHz, which is well within the capabilities of the 256MHz digitizer. For us, the IQ modulator serves as a way to cancel the noise of our source input. Once the signal passes through the IQ modulator, it is amplified, and then sent through a low pass filter. The subsequent signal goes through an analog to digital converter (ADC) and then finally the digital signal is fast fourier transformed (FFT). Then, some DSP is used to characterize the noise. The homodyne setup is seemingly simple but quite powerful.

## VIII. CONCLUSION

The design and construction of the cryostat was proven to work up to the 4K stage. The typical cooldown time for the 4K stage is approximately 30 hours, and a standard final temperature is 2.6K. The milliKelvin stage has been designed and simulated in SolidWorks and python and is expected to reach base temperature of 250mK or below. Due to long lead times in manufacturing, the stage has not been constructed and tested. The sorption fridge was successfully added to the 4K stage and has been proven to work and reach base temperatures on its ultra cold stage of roughly 250mK. A device sent from Stanford, a Niobium MKID resonator, was tested within the cryostat. Since the final milliKelvin stage was not yet setup, the Stanford device was connected directly to the ultra cold stage. The device was shown to shift its resonant frequency and quality factor as expected due to varying the temperature of the MKID by either varying the ultra cold stage temperature or varying the input power to the device. Finally, a homodyne noise characterization circuit was designed, but has yet to be constructed and tested. The cryostat will be used in the future as a testbed for astronomical instrumentation, with a heavy focus on superconducting resonators such as MKIDs. Many devices only require the 4K stage to be

tested, while others require the 250mK stage. Once the milliKelvin stage is constructed in the cryostat, then the cryostat construction will be completed, and many graduate, undergraduate, faculty and collaborators will use the system to test their devices. The finishing of the cryostat allows researchers to run many tests simultaneously, on various devices with varying critical temperatures for superconductivity.

#### ACKNOWLEDGMENT

I would like to thank Dr. Groppi and especially Dr. Mauskopf for being members of my thesis committee. I greatly appreciate the opportunity Dr. Mauskopf gave me to join his research lab and to work with many of the expensive devices, tools and instruments. None of this would have been possible without his generosity and leadership throughout my time in his lab. The opportunity he granted me has taught me a lot about performing scientific research and scientific instrumentation.

I would also like to thank Hamdi Mani. Hamdi was instrumental in getting the cryostat up and running. He spent many hours helping me get the system ready and working, as well as teaching me many skills in the laboratory including but not limited to, soldering, wirebonding, and python coding.

Lastly, I would like to thank Sean Bryan. He helped me greatly with the coding for the data analysis portion of the thesis. His assistance was pivotal to the curve fitting of the  $S_{21}$  data.

#### REFERENCES

- [1] Jacob W Kooi. Caltech. "Thermal Conductivity Integral for Stainless Steel"
- [2] Adam L. Woodcraft, et al. "Thermal Conductivity Measurements of Pitch-Bonded Graphites at milliKelvin Temperatures: Finding a Replacement for AGOT Graphite" Cryogenics, Volume 49, Issue 5, p. 159-164. 05/2009 Elsevier Ltd.
- [3] Edward Schroeder. "Superconducting Nanowire Resonators" Dec. 8, 2016.
- [4] Dr. Phil Mauskopf. "Transition Edge Sensors and Kinetic Inductance Detectors in Astronomical Instruments" (In Prep)